Fast-ion-beam laser spectroscopy of CO_2^+: Laser-induced fluorescence of the $\tilde{A}\,^2\Pi_u - \tilde{X}\,^2\Pi_g$ electronic transition

M. Larzillière, J. Lacoursière,* M. Chafik el Idrissi, N. Varfalvy, and P. Lafleur
Laboratoire de Physique Atomique et Moléculaire, Département de Physique, Université Laval, Cité Universitaire, Québec, Canada G1K 7P4

A. J. Ross
Laboratoire de Spectrométrie Ionique et Moléculaire, Université de Lyon I, 43 boulevard du 11 Novembre 1918, 69622 Villeurbanne CEDEX, France
(Received 18 September 1992)

Laser-induced fluorescence of a fast beam is obtained for a triatomic molecular ion. We use CO_2^+ in its (0,0,0) $\tilde{A}\,^2\Pi_u$–(0,0,0)$\tilde{X}\,^2\Pi_g$ electronic transition to show the feasibility of the experimental method. The high resolution (0.008 cm^{-1}) allows us to improve the accuracy of the molecular parameters of the upper (0,0,0) $^2\Pi_u$ vibronic state. Fourier-transform emission spectroscopy was used to confirm the calibration in wave numbers and the rotational analysis.

PACS number(s): 33.50.−j, 35.20.−i

INTRODUCTION

Fast-ion-beam laser spectroscopy (FIBLAS) is a very powerful high-resolution spectroscopic technique for the study of molecular-ion structure. A large number of different molecular species can be probed systematically and in various manners with FIBLAS methods [1]. They have to be far more efficient and powerful at studying ions than conventional dispersion spectroscopy techniques using Penning ionization or conventional discharges.

Laser-induced fluorescence [2] (LIF) constitutes one method that can be used successfully for detecting resonances in FIBLAS experiments. However, the detection of fluorescence coming from an ion beam is not an easy task in itself. First of all, the very low density of ions generates a rather weak fluorescence signal. It is therefore essential to use an apparatus that produces sufficiently intense beams even if the high density of photons supplied by laser radiation compensates for this low density of particles. Secondly, the LIF is always spread over a certain distance from the point where the ion-laser beam interaction begins. The distance over which the LIF is spread, depends upon the lifetime of the excited state. Ideally, the detection system should respond to fluorescence over the entire emission zone. However, the dimensions of typical photon detectors used in atomic or molecular emission experiments limit the distance over which emission can be observed to an order of a few centimeters. The transitions best suited to this technique are therefore those for which the upper-state lifetime is short, thus giving rise to emission over a distance matched by the detectors. Finally, in the cases where the ion under study is a molecule, the high density of rotational and vibrational levels leads to a very low population for such a level. The LIF signal is therefore very weak in comparison with the situation where an atomic beam is used. This is why the first LIF experiments using FIBLAS were carried out with atoms [3,4]. LIF experiments involving diatomic molecular-ion beams were later attempted successfully, namely, with the N_2^+ ion [5].

In this article, we report the observation of laser-induced fluorescence of a triatomic molecular beam, namely, CO_2^+ molecules. Spectroscopy of the CO_2^+ ion is of interest in astrophysics since emission has been observed from Mars, Venus, and also from comet tails. With the experimental setup described below, we studied with UV light the (0,0,0)-(0,0,0) band of the $\tilde{A}\,^2\Pi_u - \tilde{X}\,^2\Pi_g$ system of CO_2^+. This experiment is a prelude to a future two-photon experiment where the second photon enters in resonance with the $\tilde{C}\,^2\Sigma_g^+ - \tilde{A}\,^2\Pi_u$ visible transition, the $\tilde{C}\,^2\Sigma_g^+$ state being completely predissociated [6]. Optical-optical double-resonance spectroscopy of a fast molecular ion has already been performed by Cosby and Helm [7].

EXPERIMENT

In our FIBLAS experimental setup, depicted in Fig. 1, the ion and laser beams are collinear and parallel or antiparallel. The CO_2^+ ions are produced by a radio-frequency discharge source (RFS) and are immediately accelerated at energies between 4 and 20 keV by an Einzel gap (EG). Apart from accelerating the ions, the Einzel gap has an important focusing function because the beam coming out of the radio-frequency source is quite divergent. Since the ion source produces chemical species other than CO_2^+, chemical purity of the beam is required and is achieved via magnetic analysis performed in the horizontal plane by an electromagnet (MA1). The correct alignment of the ion beam in the vertical plane is obtained by means of two deflecting plates (DP), while an Einzel lens (EIN) and slits (S) permit optimum focusing of the beam at the entrance of the analyzing magnet (MA1). At the exit of magnet MA1, a triplet of quadrupolar lenses (TQ) focuses the CO_2^+ beam on a Faraday

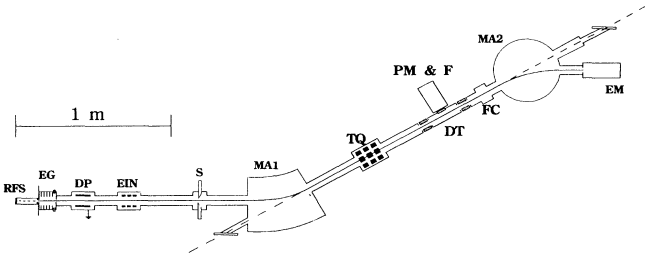

FIG. 1. FIBLAS experimental setup. RFS, radio-frequency discharge source; EG, Einzel gap; DP, deflecting plates; EIN, Einzel lens; S, slits; MA1, magnet analyzer; TQ, triplet of quadrupolar lens; DT, Doppler tuning zone; PM, photomultiplier tube; F, filter; FC, Faraday cup; MA2, magnet analyzer; EM, electron multiplier.

cup (FC) situated after a Doppler tuning zone (DT). This zone, which defines spatially the ion-laser beam interaction, consists of a drift tube which is an electrically isolated section of the beam line on which a tunable voltage is applied. It allows Doppler tuning of the molecular transition of interest with a fixed laser wavelength. Scanning the applied voltage changes the speed of the ions which is thus equivalent to scanning the laser wavelength. The tunable voltage covered 1 kV, and the accelerating field was incremented by 0.5 kV between each scan to ensure good overlap between consecutive spectra. An ionization gauge placed near the drift tube indicates a residual gas pressure of 7×10^{-8} Torr. Typically, we measure a 5 μA current in our experiments on the Faraday cup located beyond the drift tube.

The laser radiation is supplied by an Ar^+ cw laser (model Innova 200-25/5 from Coherent) tuned to the 351.112-nm line and operated in a single mode by means of an intracavity Fabry-Pérot etalon. The laser power in the drift tube is about 200 mW. The spectral width of the monomode laser line is known to be less than 20 MHz [2].

The LIF signal is detected with a photomultiplier tube (PM) used in a counting mode and cooled to about -15 °C. The photomultiplier is placed on the drift tube, perpendicularly to the beam line and at a distance of a few centimeters in front of the drift tube. The use of an interference filter (F) centered at 400.0 nm and having a full width at half maximum (FWHM) of 10 nm prevents the 351.112-nm laser radiation from generating too much noise in the photomultiplier tube, which is always one of the main problems in LIF experiments, given the small signals involved. Simultaneously, this filter allows the detection of the

$$(0,0,0)\,\tilde{A}\,^2\Pi_u-(0,0,0)\tilde{X}\,^2\Pi_g$$

resonances by being transparent to the LIF photons emitted from the (0,0,0) $\tilde{A}\,^2\Pi_u$ state down to the excited vibrational levels of the $\tilde{X}\,^2\Pi_g$ state. At the end of the beam line, a second analyzing electromagnet (MA2) and an electron multiplier (EM) may be used to mass-analyze the ion beam in order to make sure the chemical species accelerated is the right one. This operation is not necessary in the present experiment, the mass 44 of CO_2^+ being easy to isolate without ambiguity. The electromagnet and the electron multiplier may also be used to detect molecular or atomic fragments when a predissociation process allows the detection of resonances via photofragment counting, although this was not done in the experiment described here. Two Brewster windows, one at each end of the beam line, prevent multiple back-and-forth reflections of the laser beam which would occur on windows orthogonal to the beam line. This would increase the background noise in the spectra because the interference filter is not 100% efficient at cutting the laser light. The Brewster window near magnet MA1 also minimizes laser-power loss.

The spectrum obtained with the experimental setup described above is shown in Fig. 2. Some rotation lines of the (0,0,0)-(0,0,0) band of the $\tilde{A}\,^2\Pi_{u,1/2}-\tilde{X}\,^2\Pi_{g,1/2}$ system are assigned according to the results of Mrozowski [8]. The unidentified weaker lines come from hot bands of the same electronic system and are very sensitive to the radio-frequency discharge regime. Indeed, some of them disappear completely from the spectrum under slight changes of the discharge regime. The presence of all these hot bands complicates the task of the spectroscopist, but it is of course precisely this ability of the radio-frequency ion source to produce excited molecular species that allows us to study the $\tilde{A}\,^2\Pi_{u,1/2}-\tilde{X}\,^2\Pi_{g,1/2}$ system of CO_2^+, the lower electronic level of this resonance lying 160 cm^{-1} above its lowest level of the ground state. The FWHM of the observed lines is about 230 MHz. This width originates essentially from the measured $\pm$4-V ripple tension of the accelerator. The contribution to linewidth from the energy spread of the source is much smaller. The background noise is mainly produced by collisions between the ion beam and the residual gas in the drift tube.

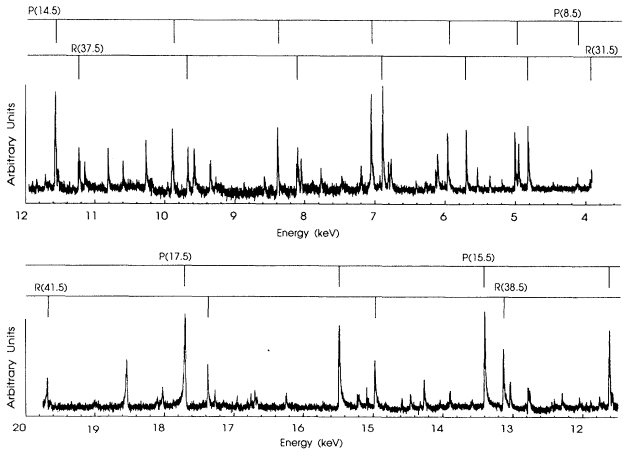

FIG. 2. Laser-induced fluorescence spectrum obtained with a fast ion beam of CO_2^+ between 4 and 20 keV. The exciting laser line and the ion beam are parallel. In the calculation of the Doppler shift, we used the wave number 28 472.810 cm^{-1} for the 351.112-nm Ar^+ line (even if the last digit is not available in the literature).

The acknowledged drawback associated with the FIBLAS technique is that while differences between line positions in a given spectrum can be measured very accurately, absolute calibration is lacking. The difficulty arises from the need to measure an accelerating electric field of several kV with high precision, and from an uncertainty in the potential within the ion source. The technical problem of measuring the electric field precisely has been considered by Holt *et al.* [9] via the use of parallel and antiparallel configurations and a tunable laser. However, with our single-frequency ion-laser experiment, we cannot use this method, and we therefore need a reference spectrum with independent calibration so as to set our entire FIBLAS spectrum on an absolute scale. As there were no reliable data (see text below) for these bands of CO_2^+ available in the literature, we recorded the emission spectrum of CO_2^+ produced by a low-pressure, water-cooled discharge lamp on a Fourier-transform spectrometer. This spectrometer is calibrated by a frequency-stabilized single-mode He-Ne laser, but systematic errors in absolute calibration can be introduced if the optical alignment of the external emission source with the interferometer is imperfect. We therefore used atomic emission lines present in the source to check the absolute calibration of the FT spectrometer in the spectral region of interest, and from these the precision in absolute line position is found to be 0.02 cm^{-1}. We went on to record the emission bands of CO_2^+ in the region 27 000–30 000 cm^{-1} at an instrumental resolution of 0.08 cm^{-1}. In our low-pressure discharge source, the pressure is less than 10^{-4} Torr and the temperature about 150 °C; the Doppler width is estimated to be 0.063 cm^{-1}. Part of the Fourier-transform emission spectrum is reproduced in Fig. 3. The upper and lower traces correspond to the

$$(0,0,0)\tilde{A}\,^2\Pi_{u,1/2}-(0,0,0)\tilde{X}\,^2\Pi_{g,1/2}$$

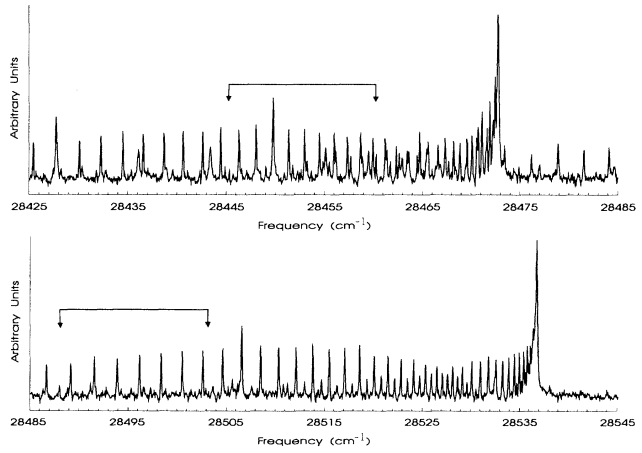

FIG. 3. FT emission spectra of CO_2^+. The upper and lower spectra are, respectively, the subbands $(0,0,0)\tilde{A}\,^2\Pi_{u,1/2}-(0,0,0)\tilde{X}\,^2\Pi_{g,1/2}$ and $(0,0,0)\tilde{A}\,^2\Pi_{u,3/2}-(0,0,0)\tilde{X}\,^2\Pi_{g,3/2}$. The two arrows show the limits of the spectrum recorded by FIBLAS. These spectra were recorded on a BOMEM DA3 interferometer (Corning filter 7-60, 1052 scans, resolution of 0.08 cm^{-1}, photomultiplier EMI S20 as detector).

and

$$(0,0,0)\tilde{A}\,^2\Pi_{u,3/2}-(0,0,0)\tilde{X}\,^2\Pi_{g,3/2}$$

subbands, respectively. The arrows indicate the limits of the spectrum recorded by the FIBLAS technique.

In Fig. 4 we present two LIF spectra with different resolution for a spectral region ($\cong 1.2$ cm^{-1}) corresponding to one of our 1-kV scans on the drift tube, the accelerating field being 8 kV. The upper one is obtained with the multimode laser line, and the lower one with the single-mode laser line. These spectra illustrate two experimental points. First, the accelerator was stable throughout the two hours required to select a single laser mode. Second, it can be seen from the lower spectrum in Fig. 4 that only one laser mode was selected, so there was no need to include a UV mode analyzer in the experimental setup. The width of the multimode UV laser line could be accurately measured on the upper spectrum. The full width is 9.62 GHz and the FWHM is 5.64 GHz.

Figure 5 shows two spectra, the upper one obtained by FIBLAS, and the lower one by FT emission spectroscopy. They offer a comparison between the resolution due to the kinematic compression of the velocity distribution and the resolution limited by the Doppler effect. A comparison is possible because CO_2^+ has no hyperfine structure. These two spectra represent the spectral region between 28 500.95 and 28 488.22 cm^{-1}. For the sake of clarity, we adopted a scale in keV because the FIBLAS

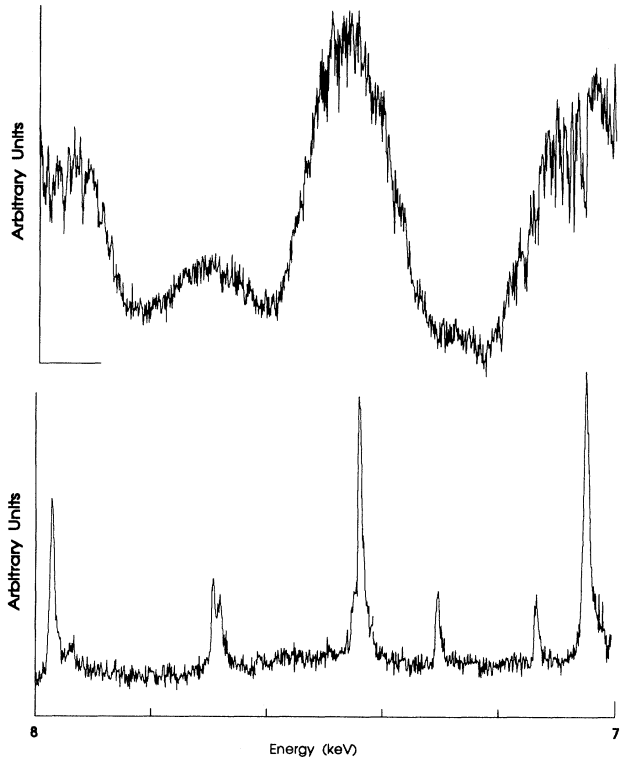

FIG. 4. Top, LIF spectrum with the multimode laser line; bottom, LIF spectrum with the monomode laser line.

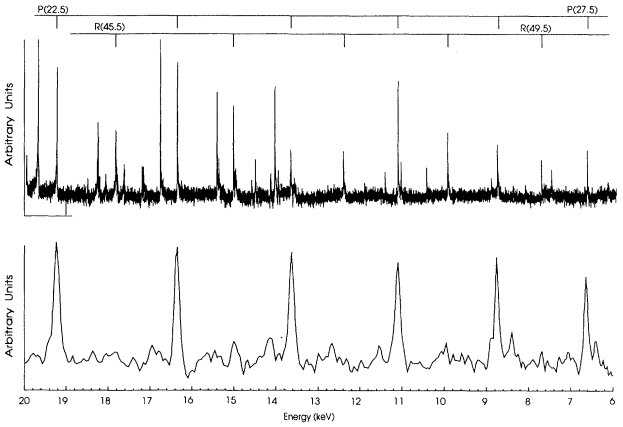

FIG. 5. These two spectra represent the spectral region between 28 500.95 and 28 488.22 cm^{-1}. Top, LIF spectrum obtained with a fast ion beam of CO_2^+ antiparallel to the laser. In the calculation of the Doppler shift, we used the wave number 28 472.810 cm^{-1} for the 351.112-nm Ar^+ line. Bottom, FT emission spectrum composed principally of P lines of the $(0,0,0)\,\tilde{A}\,^2\Pi_{u,3/2}-(0,0,0)\tilde{X}\,^2\Pi_{g,3/2}$ subband [$P(22.5)$ to $P(27.5)$].

spectra are recorded in keV and because the frequency scale is very nearly linear in keV for the scan lengths and the beam energies which apply here. The lower FT emission spectrum is composed principally of P lines of the

$$(0,0,0)\,\tilde{A}\,^2\Pi_{u,3/2}-(0,0,0)\tilde{X}\,^2\Pi_{g,3/2}$$

subband [$P(22.5)$ to $P(27.5)$]. The upper FIBLAS spectrum shows more rotational lines coming from hot bands, mostly from the

$$(0,1,0)\,\tilde{A}\,^2\Sigma_u^+-(0,1,0)\tilde{X}^2\Sigma_g^+$$

band. This spectrum is obtained with the laser beam antiparallel to the ion beam. We must point out that the relative intensity of the rotational lines is not totally reliable, because the whole spectrum is composed of several spectra of 1-kV scan, and the intensity of the molecular beam depends strongly on the accelerating field. For a 5-μA ion beam, a typical signal of 1000 counts per second is recorded. The intensity scales for all the spectra given in the figures are arbitrary.

RESULTS AND DISCUSSION

As mentioned before, CO_2^+ is interesting for astrophysics and space, but also for molecular physics because it belongs to the family of linear triatomic molecules having 15 valence electrons and exhibiting a Renner-Teller effect in its $\tilde{X}\,^2\Pi_g$ ground state. For these reasons, much work has been done on this radical. Unfortunately, its first electronic transition $\tilde{A}\,^2\Pi_u-\tilde{X}\,^2\Pi_g$ lies in the UV, which precludes the use of a powerful cw tunable laser.

The first emission work under high resolution and the first rotational analysis were done by Mrozowski [8]. Many bands involving the stretching vibrational mode of the $\tilde{A}$-$\tilde{X}$ system were analyzed. Gauyacq *et al.* [10] were the first to analyze the bending vibrational mode of this system and to give an interpretation of the Renner-Teller effect on the two electronic states. The first experimental work with a pulsed laser was done by Bondybey and Miller [11] where they reported the first rotationally resolved laser excitation spectra of a polyatomic ionic species. Later, Erman *et al.* [12] found new perturbations in the (0,0,0) and (1,0,0) vibrational levels of the $\tilde{A}\,^2\Pi_u$ state. At the same time, Johnson *et al.* [13] published the first work using laser spectroscopy devoted to the $\tilde{B}$-$\tilde{X}$ transitions to show the interaction between the (0,0,0) $\tilde{B}$ level and vibronic levels of the $\tilde{A}$ state. More recently, Frye and Sears [14] measured the Renner-Teller effect in the $\tilde{X}\,^2\Pi_g$ state by infrared diode laser absorption. Due to a reduced Doppler effect in the infrared, these authors were able to obtain precise rotational constants, which were used by Larzillière and Jungen [15] for a complete treatment of the effects of angular momentum and vibrational anharmonicity of the $\tilde{X}\,^2\Pi_g$ state.

In this paper we present the first highly resolved spectrum of the UV $\tilde{A}$-$\tilde{X}$ transition of CO_2^+ (0.008-cm^{-1} resolution in this spectral region represents a resolvance of 3.5×10^6). Such a resolution provides a complete view of the rotational structure of the molecule.

For example, the staggering effect (see Herzberg [16], p. 267) observed for a symmetric molecule having a zero nuclear spin for which half of the rotational transitions are missing is clearly shown. The separation between neighboring P and R rotational lines is not usual (e.g., $P(15.5)$, $R(38.5)$ and $P(16.5)$, $R(39.5)$]. Also, the separation between two consecutive R and/or P lines does not increase normally with the rotational quantum number J.

The observed rotational transitions are classified in Table I in four branches for each of the two subbands. The precision of the relative positions of the rotational transitions is 0.009 cm^{-1} for the FT emission spectrum and 0.003 cm^{-1} for the FIBLAS spectrum. For the two experiments the absolute frequency precision is 0.02 cm^{-1} (see text above). The lines which were observed both by FIBLAS and in the FT emission spectra are indicated by a footnote b. Lines observed only by FIBLAS are indicated by a footnote c.

The reduction of the line positions in terms of molecular constants is obtained by using the matrix elements of Table II. They represent the rotational energy levels of the two $^2\Pi$ (0,0,0) vibronic states. In a linear triatomic molecule belonging to coupling case a, the rotational energy-level matrix elements must account for the fact that the rotational-vibrational motion is not separable from the electronic motion [17]. However, the levels having $v_2=K-1$ ($v_2=0$, $K=1$) are the so-called unique levels [17]. Each of these levels is represented approximately by a single spin pair of basis functions

$$|v_2,l=K-1,\Lambda=+1,\Sigma=\pm\tfrac{1}{2}\rangle$$

for a given (signed) value of $K=l+\Lambda$, the quantum number l being the pure nuclear angular-momentum component along the Z axis associated with the bending vibration and Λ the (signed) projection of the electronic angular momentum along the same axis. These rotational-energy-level matrix elements, including centrifugal dis-

TABLE I. Wave numbers of the rotational transitions in cm^{-1}.

$J-0.5$	R_{ff}	R_{ee}	P_{ff}	P_{ee}
		$(0,0,0)\tilde{A}\,^2\Pi_{u,3/2}-(0,0,0)\tilde{X}\,^2\Pi_{g,1/2}$		
0				
1			28 467.175	
2		28 470.497		28 466.349
3	28 471.026[a]		28 465.375	
4		28 471.405		28 464.390
5	28 471.819[a]		28 463.386	
6				28 462.269
7	28 472.369[a]		28 461.126	
8		28 472.516[a]		28 459.889
9	28 472.670[a]		28 458.626	
10				28 457.252
11			28 455.904	
12		28 472.670[a]		28 454.401[c]
13			28 452.912[c]	
14		28 472.369[a]		28 451.299[c]
15	28 472.183		28 449.710[c]	
16		28 471.819[a]		28 447.966[c]
17	28 471.542		28 446.248[c]	
18		28 471.026[a]		28 444.378
19	28 470.652		28 442.554	
20		28 470.020		28 440.547
21	28 469.512		28 438.616	
22		28 468.772		28 436.484
23	28 468.137		28 434.430	
24		28 467.172		28 432.163
25	28 466.513		28 429.993	
26		28 465.516		28 427.629
27	28 464.646		28 425.339	
28		28 463.511		
29	28 462.269			
30		28 461.306		
31	28 460.197			
32		28 458.619		
33	28 457.602			
34		28 456.091		
35	28 454.776[b]			
36		28 453.138[b]		
37	28 451.701[b]			
38		28 449.936[b]		
39	28 448.383[b]			
40		28 446.491[b]		
41	28 444.823[b]			
		$(0,0,0)\tilde{A}\,^2\Pi_{u,3/2}-(0,0,0)\tilde{X}\,^2\Pi_{g,3/2}$		
0				
1	28 534.115		28 531.280	
2		28 534.610		28 530.428
3	28 535.083		28 529.514	
4		28 535.521		28 528.538
5	28 535.866		28 527.503	
6		28 536.178		28 526.401
7			28 525.248	
8		28 536.563[a]		28 524.029
9	28 536.672[a]		28 522.724	
10				28 521.362
11			28 519.961	
12		28 536.625[a]		28 518.498
13			28 516.957	
14		28 536.340[a]		28 515.385

Table I. *(Continued).*

$J-0.5$	R_{ff}	R_{ee}	P_{ff}	P_{ee}
15	28 536.018		28 513.708	
16		28 535.693		28 511.997
17	28 535.298		28 510.214	
18		28 534.867		28 508.376
19	28 534.347		28 506.452	
20		28 533.769		28 504.499
21	28 533.132		28 502.474	
22		28 532.436		28 500.396[c]
23	28 531.705		28 498.236[c]	
24		28 530.880		28 496.020[c]
25	28 529.985		28 493.737[c]	
26		28 529.031		28 491.406[c]
27	28 528.034		28 489.002[c]	
28		28 526.978		28 486.558
29	28 525.862		28 484.032	
30		28 524.650		28 481.432
31	28 523.377		28 478.794	
32		28 522.055		
33	28 520.679			
34				
35	28 517.781			
|				
45	28 499.365[b]			
46		28 497.175[b]		
47	28 494.947[b]			
48		28 492.632[b]		
49	28 490.282[b]			

[a]Overlapped line position.
[b]Observed only in FIBLAS spectrum.
[c]Observed in FT and FIBLAS spectra.

tortion, K-type doubling, and spin-rotation interaction, are commonly used by other authors [18–20]. In Ref. [20], a factor $(-1)^{J-1/2}$ was incorporated into the K-type doubling term. This factor corrects for the fact that lines are missing due to the nuclear spin statistics, and the four branches are grouped in two for each subband, as was done by Mrozowski [8]. Such a procedure is not commonly used.

The usual molecular constants ν_0, B, D, γ, p, and q (defined in Refs. [16] and [18]) have been obtained through least-squares fitting of the measured line positions to the appropriate expressions in Table I. Three data sets were treated separately. They were (i) the data given by Mrozowski [8], (ii) the data from the emission experiment recorded with the FT interferometer, and (iii) the high-resolution FIBLAS data. All the molecular parameters are summarized in Table III.

First we must point out that there is quite a difference between our ν_0 value and the previous one. This is because the absolute calibration of our FT emission spectrum is better than that of the photographic plate used in the earlier work. Although it is difficult to measure the accelerating field in a FIBLAS experiment with precision, and to determine the plasma shift exactly (see Ref. [21]),

TABLE II. The two (e and f) 2×2 energy matrices of the $^2\Pi$ state. The upper and the lower signs refer to e and f components, respectively; the parameter T includes ε and γ. $X=(J+\frac{1}{2})^2-K^2$.

$^2\Pi^{e,f}_{1/2}$	$^2\Pi^{e,f}_{3/2}$
$T_{v=0,K=1,\Sigma=-\frac{1}{2}}+B(X+1)$	$-(B-\frac{1}{2}\gamma)\sqrt{X}+2DX\sqrt{X}-\frac{1}{4}p\sqrt{X}$
$-D[(X+1)^2+X]-\frac{1}{2}p[-1\pm\sqrt{(X+1)}]$	$+\frac{1}{2}q\sqrt{X}[-1\pm\sqrt{(X+1)}]$
$-\frac{1}{2}q[-(X+2)\pm2\sqrt{(X+1)}]$	
Symmetric	$T_{v=0,K=1,\Sigma=+\frac{1}{2}}+B(X-1)$
	$-D[(X-1)^2+X]-\frac{1}{2}qX$

TABLE III. Molecular constants obtained from the rotational analysis of the (0,0,0)-(0,0,0) $\tilde{A}$-$\tilde{X}$ bands of CO_2^+ in cm^{-1}. $\nu_0=\frac{1}{2}(T'_{v'k'\Sigma'=+\frac{1}{2}}+T'_{v'k'\Sigma'=-\frac{1}{2}})-\frac{1}{2}(T''_{v''k''\Sigma''=+\frac{1}{2}}+T''_{v''k''\Sigma''=-\frac{1}{2}})$ and $A=(T_{vk\Sigma=-\frac{1}{2}}-T_{vk\Sigma=\frac{1}{2}})$ (Ref. [15]).

$\tilde{X}\,^2\Pi_g$	Ref. [10]	Ref. [14]	FT
ν_0	0.0	0.0	0.0
A	−159.917(5)	−151.598	−159.598
B	0.3802(1)	0.380 506(15)	0.380 53(1)
10^7D	0.96(25)	1.36(13)	1.4(1)
10^3p	3.0(3)	3.9(1.9)	5.4(3)
10^5q	−4.67[a]	−5.12(94)	−4.4(7)
$10^3\gamma$			1.0(8)
$\tilde{A}\,^2\Pi_u$	Ref. [10]	FT	FIBLAS
ν_0	28 500.52(1)	28 500.350(2)	28 500.350(9)
A	−95.86(1)	−95.512(3)	−95.512(8)
B	0.349 71(1)	0.349 90(1)	0.349 94(4)
10^7D	0.91(4)	1.29(8)	1.4(2)
10^3p	6.2(3)	8.8(2)	8.4(2)
10^5q	−4.60[a]	−3(2)	−3[b]
$10^3\gamma$		1.1(5)	1.1[b]
σ	0.030	0.0097	0.0094

[a]Calculated.
[b]Kept fixed.

we estimate that a precision of about 50 V can be obtained with our experimental setup. Any discrepancy between the real and the measured tension is the same for any molecular or atomic ion in the source and will lead to some systematic shift on line positions, but even so, an error of 50 V corresponds to an error of about 0.05 cm^{-1} which is much smaller than the original discrepancy of about 0.135 cm^{-1} between the ν_0 values in [8] and the new FT data. In Table III the standard deviation quoted for ν_0 is determined from the least-squares-fitting procedure, and does not reflect the experimental precision.

Due to the lack of rotational transitions (half of the lines are missing), K-type doubling parameters for both electronic states are difficult to determine because they are correlated to one another and to the rotational constants B and D. Nevertheless, the quality of our data and the number of observed lines in the FT spectrum minimized this effect. These parameters are in good agreement with those given by Gauyacq *et al.* [10]. For the ground state, they are in very good agreement with those resulting from the IR laser absorption work of Frye and Sears [14].

Spin-rotation parameters γ are given for the two electronic states. Our fitting procedure gives the values 1.0×10^{-3} and 1.1×10^{-3} cm^{-1} for the lower and upper state, respectively. These values are about the same as those for NCO [19] and N_2O^+ [15]. These two parameters are strongly correlated to one another and were determined separately. In other words, one of the γ parameters is kept fixed in each fit and at each time this last one is varied by steps of $\pm0.1\times10^{-3}$ cm^{-1}. The resulting values given in Table III correspond to the lowest standard deviation σ obtained in that way. During the fit of the FIBLAS data, these parameters were kept fixed.

We found that the second-order spin-orbit parameters A_J were not significant. Sometimes these parameters can be used to reveal a difference between the rotational constants of the two substates $\Pi_{1/2}$ and $\Pi_{3/2}$. That is not the case for CO_2^+. Larzillière and Jungen [15] also showed clearly that these rotational constants are identical for the ground state (B_{obs}, 0.380 506 cm^{-1}; B_{calc}, 0.380 52 cm^{-1}).

Our spectra also reveal a weak hot band lying around 28 460 cm^{-1} and overlapped by the $\tilde{A}\,^2\Pi_{u,1/2}$–$\tilde{X}\,^2\Pi_{g,1/2}$ subband. At present, we are not able to assign these rotational transitions with no obvious structure. At first, we tried to use the published bands assigned previously but only a few rotational lines with very high J seemed to be present. This work is in progress.

CONCLUSION

Laser techniques have been used to record a very highly resolved UV spectrum of CO_2^+. Also, laser-induced fluorescence results using the FIBLAS technique for a triatomic ion have been given. This preliminary work opens the door to new experiments on CO_2^+, which is an interesting triatomic ion for several domains of physics.

Although the ground state has been studied to understand the Renner-Teller effect, little is known about the first excited state $\tilde{A}\,^2\Pi_u$. The FIBLAS technique is well suited to study the rovibronic structure of this state.

Also, following the two-photon absorption work of Wyttenbach, Evard, and Maier [6], this first result in LIF shows the possibility of adapting the two-photon absorption spectroscopy to a fast ion beam, because the $\tilde{C}\,^2\Sigma_g^+$ state is governed by a slow predissociation. In that case, the photofragments provide a highly efficient indirect detection method. The method is particularly valuable in

this instance because the *u-g* selection rule means that the $\tilde{C}\,^2\Sigma_g^+$ state is not accessible from the ground electronic state $\tilde{X}\,^2\Pi_g$ with a one-photon transition.

ACKNOWLEDGMENTS

The authors would like to thank Professor R. Bacis for his help in the FT emission work and also Dr. Ch. Jungen for helpful discussions. This work was supported by the National Science and Engineering Research Council of Canada, and the FT interferometer in Lyon was financed by the CNRS Université Lyon I and the Région Rhone Alpes. The Laboratoire de Spectrométrie Ionique et Moléculaire is "Unité de recherche associée au CNRS No. 171."

*Present address: LURE, Bâtiment 209d, Université Paris–Sud, 91405 Orsay CEDEX, France.

[1] M. Dufay and M. L. Gaillard, *Laser Spectroscopy III,* Proceedings of the Third International Conference, Wyoming, edited by J. Hall and J. L. Carsten (Springer-Verlag, New York, 1977).

[2] W. Demtröder, *Laser Spectroscopy: Basic Concepts and Instrumentation,* Springer Series in Chemical Physics Vol. 5 (Springer-Verlag, New York, 1981).

[3] H. J. Andrä, A. Gaupp, and W. Wittmann, Phys. Rev. Lett. **31**, 501 (1973).

[4] S. L. Kaufman, Opt. Commun. **17**, 309 (1976).

[5] S. D. Rosner, T. D. Gaily, and R. A. Holt, Phys. Rev. A **26**, 697 (1982).

[6] T. Wyttenbach, D. D. Evard, and J. P. Maier, J. Chem. Phys. **90**, 4645 (1989).

[7] P. C. Cosby and H. Helm, J. Chem. Phys. **76**, 4720 (1982).

[8] S. Mrozowski, Phys. Rev. **60**, 730 (1941); **62**, 270 (1942); **72**, 682 (1947); **72**, 691 (1947).

[9] R. A. Holt, S. D. Rosner, T. D. Gaily, and A. G. Adam, Phys. Rev. A **22**, 1563 (1980).

[10] D. Gauyacq, C. Larcher, S. Leach, and J. Rostas, Can. J. Phys. **53**, 2040 (1975); D. Gauyacq, C. Larcher, and J. Rostas, *ibid.* **37**, 684 (1979); C. Larcher, D. Gauyacq, and J. Rostas, J. Chim. Phys. **77**, 655 (1980).

[11] V. E. Bondybey and T. A. Miller, J. Chem. Phys. **67**, 1790 (1977).

[12] P. Erman, F. A. Grimm, A. Gustafsson, and M. Larson, Phys. Scr. **28**, 611 (1981).

[13] M. A. Johnson, R. N. Zare, J. Rostas, and S. Leach, J. Chem. Phys. **80**, 2407 (1983).

[14] J. M. Frye and T. J. Sears, Mol. Phys. **62**, 919 (1987).

[15] M. Larzillière and Ch. Jungen, Mol. Phys. **67**, 807 (1989).

[16] G. Herzberg, *Spectra of Diatomic Molecules* (Van Nostrand, Princeton, 1951).

[17] C. Jungen and A. J. Merer, Mol. Phys. **40**, 1 (1980); **40**, 95 (1980).

[18] H. Lefebvre-Brion and R. W. Field, *Perturbation in the Spectra of Diatomic Molecules* (Academic, New York, 1986).

[19] P. S. H. Bolman, J. M. Brown, A. Carrington, I. Kopp, and D. A. Ramsay, Proc. R. Soc. London Ser. A **343**, 17 (1975).

[20] T. J. Sears, Mol. Phys. **59**, 259 (1986).

[21] M. Carré, M. Druetta, M. L. Gaillard, H. H. Bukow, M. Horani, A. L. Roche, and M. Velghe, Mol. Phys. **40**, 1453 (1980).